



Recent Developments and Characterization Techniques in 3D printing of Corneal Stroma Tissue

Journal:	<i>Polymers for Advanced Technologies</i>
Manuscript ID	PAT-21-143.R1
Wiley - Manuscript type:	Research Article
Date Submitted by the Author:	04-Apr-2021
Complete List of Authors:	<p>Ulag, Songul; Marmara University - Goztepe Campus, Department of Metallurgical and Materials Engineering; Marmara University - Goztepe Campus, Center for Nanotechnology & Biomaterials Application and Research (NBUAM)</p> <p>Uysal, Ebru</p> <p>Bedir, Tuba ; Yildiz Technical University Faculty of Chemical and Metallurgical Engineering, Department of Bioengineering; Marmara University - Goztepe Campus, Center for Nanotechnology & Biomaterials Application and Research (NBUAM)</p> <p>SENGOR, Mustafa; Marmara University</p> <p>Ekren, Nazmi; Marmara Universitesi - Goztepe Kampusu</p> <p>ÜSTÜNDAĞ, Cem; Yildiz Technical University, Bioengineering; Yildiz Technical University</p> <p>Midha, Swati</p> <p>Kalaskar, Deepak</p> <p>Gunduz, Oguzhan; Marmara University - Goztepe Campus, Department of Metallurgical and Materials Engineering, Faculty of Technology; Marmara University - Goztepe Campus, Center for Nanotechnology & Biomaterials Application and Research (NBUAM)</p>
Keywords:	artificial cornea, corneal stroma, characterization, hydrogels, 3D printing

SCHOLARONE™
Manuscripts

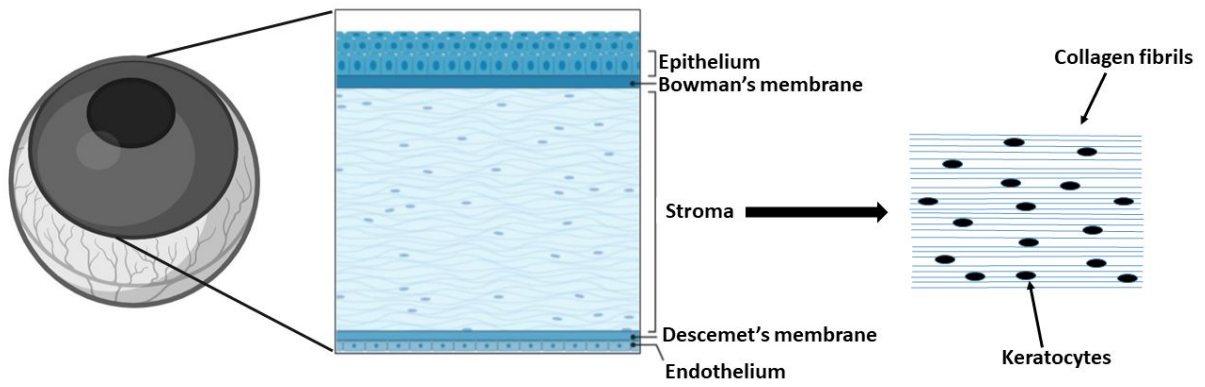


Figure 1.

For Peer Review

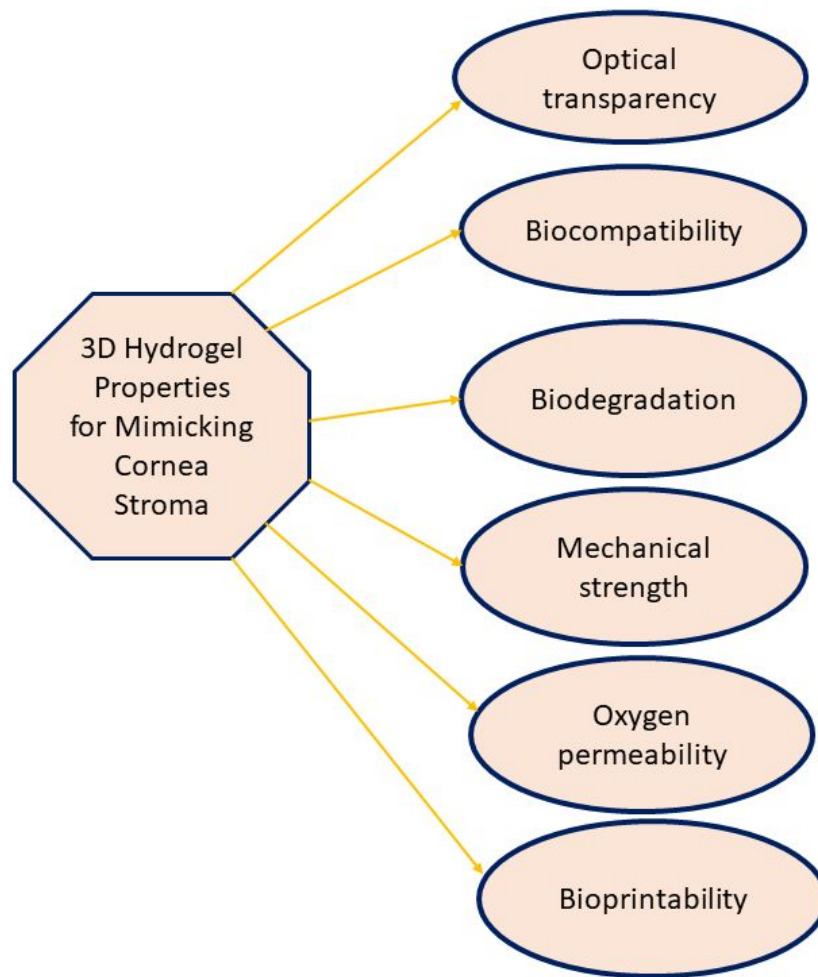


Figure 2.

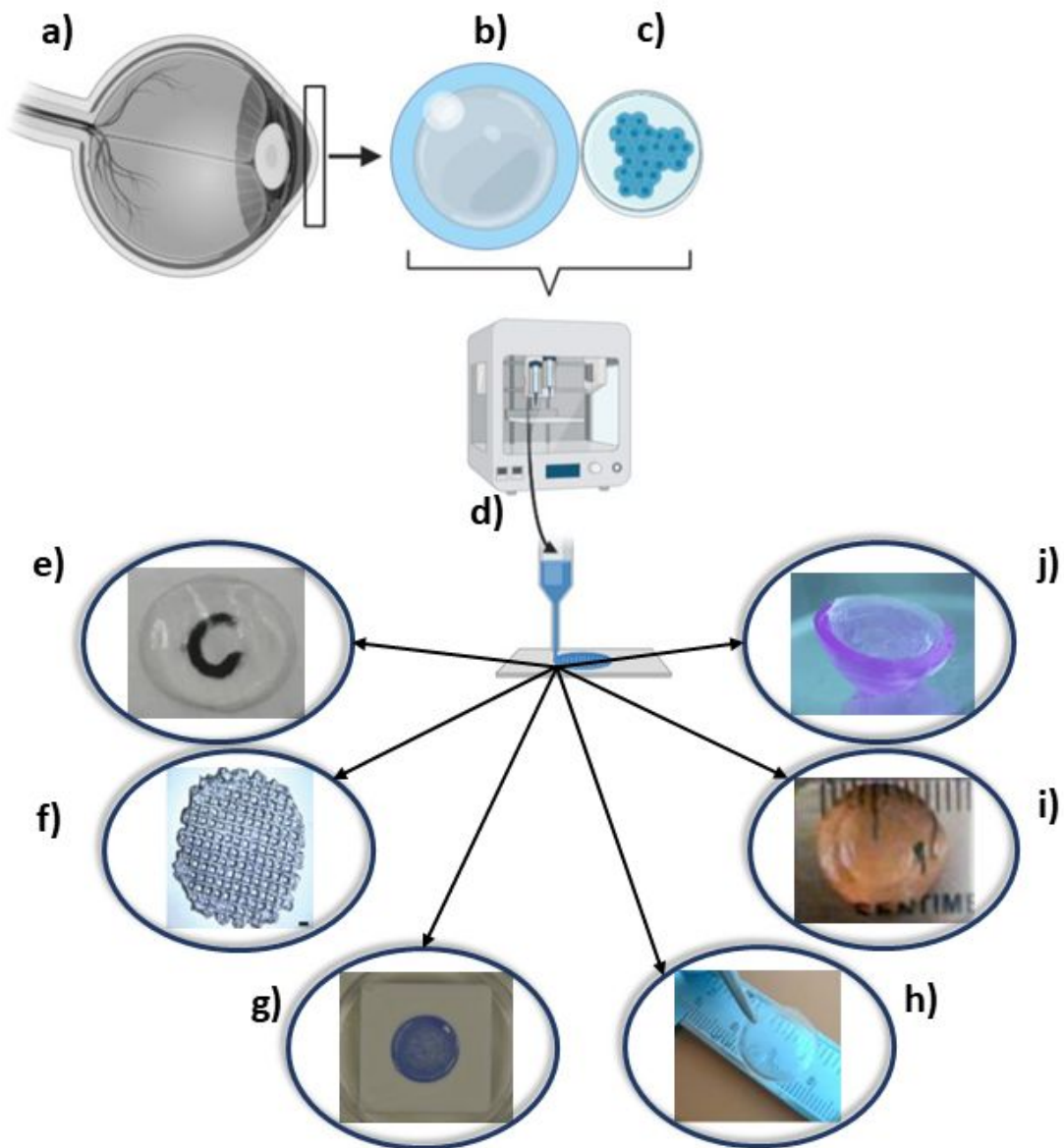


Figure 3.

Recent Developments and Characterization Techniques in 3D printing of Corneal Stroma Tissue

Songul Ulag¹, Ebru Uysal², Tuba Bedir¹, Mustafa Sengor¹, Nazmi Ekren¹, Cem Bulent Ustundag^{1,2}, Swati Midha³, Deepak M. kalaskar^{3*}, Oguzhan Gunduz^{1*}

¹Center for Nanotechnology & Biomaterials Application and Research (NBUAM), Marmara University, Turkey

²Department of Bioengineering, Faculty of Chemistry and Metallurgy, Yildiz Technical University, Turkey

³UCL Division of Surgery & Interventional Science, University College London (UCL), London, United Kingdom

*d.kalaskar@ucl.ac.uk, *ucemogu@ucl.ac.uk

Abstract

Corneal stroma has a significant function in normal visual function. The corneal stroma is vulnerable because of being the thickest part of the cornea, as it can be affected easily by infections or injuries. Any problems on corneal stroma can result in blindness. Donor shortage for corneal transplantation is one of the main issues in corneal transplantation. To address this issue, the corneal tissue engineering focuses on replacing injured tissues and repairing normal functions. Currently, there are no available, engineered corneal tissues for widely accepted routine clinical treatment, but new emerging 3D printing applications are being recognized as a promising option. Recent *in vitro* researches revealed that the biocompatibility and regeneration possessions of 3D printed hydrogels outperformed conventional tissue engineering approaches. The goal of this review is to highlight the current developments in the characterization of 3D cell-free and bioprinted hydrogels.

Keywords: artificial cornea; corneal stroma; characterization; hydrogels; 3D printing.

1. Introduction

The human cornea, a transparent and avascular tissue placed in the anterior part of the eye, has two crucial functions. It acts as the primary optical element that refracts about 75% of the incident light, and functions as a barrier to protecting the internal components of the eye against mechanical damages, UV light and infections [1, 2]. The cornea is around 11-12 mm in diameter vertically and horizontally in adults [3, 4]. The cornea comprises of three main cellular layers: the outermost epithelium, stroma and innermost endothelium. Two acellular interfaces called the Bowman's layer and Descemet's membranes (Figure 1) [5].

The corneal stroma is a collagen-rich connective tissue that composes of about 90% of the corneal thickness [6]. The collagen fibers are organized in parallel bundles called fibrils [7]. The fibrils contain highly organized collagen types I, III, V, VI, with proper alignment and spacing necessary for the transparency of the cornea [8, 9]. Aligned fibrils are packaged in

1
2
3 layers called lamellae. The corneal stroma consists of 200 to 250 distinct lamellae, and each
4
5 layer is arranged perpendicular to the fibers in adjacent lamellae [10]. This arrangement is
6
7 crucial for preserving corneal mechanical strength [11].
8
9

10 There are bridges formed by glycosaminoglycan and proteoglycans between the lamella.
11
12 Keratocytes can express keratocan, ALDH3A1 (Aldehyde dehydrogenase 3 family, member
13
14 A1), and keratan sulfate and are immobile. In corneal injuries, these immobile keratocytes can
15
16 turn into fibroblasts and myofibroblasts that can secrete randomly disturbed collagen fibrils to
17
18 repair the damage. It is critical to maintaining the vertical alignment of this lamella and the
19
20 keratocyte structure in the regeneration of the corneal tissue [12].
21
22

23
24 Corneal blindness affects over 10 million individuals worldwide [13]. Partial or full thickness
25
26 transplantation of cadaveric donor cornea, also known as keratoplasty, is the most effective
27
28 treatment for improving vision [14, 15]. However, deficiency of donor cornea is the main
29
30 limiting factor of corneal transplantation. Although approximately 130,000 corneas are donated
31
32 annually globally, most transplants result in immune rejection [16, 17]. Another treatment
33
34 choice, keratoprosthesis (KPro) implantation, involves removing the diseased cornea and
35
36 changing by an artificial cornea [18]. However, severe complications such as corneal melting,
37
38 glaucoma, prosthesis extrusion, membrane formation and calcification can occur [15, 19].
39
40

41
42 The creation of biocompatible, optically transparent and mechanically stable structures poses a
43
44 significant challenge in producing corneal replacements [20].
45
46

47 **2. Tissue engineering approaches**

48
49 Many approaches have been adopted in tissue engineerings, such as a polymer, cell, and
50
51 hydrogel-based [6]. Polymers are widely adopted due to their high surface/volume ratio, high
52
53 porosity, biodegradability and mechanical behaviours, and biocompatibility [21]. Materials
54
55 used in scaffolds can be synthetic or natural, degradable or non-degradable depending upon the
56
57 purpose of use (Table 1). Main polymers used as biomaterials include natural and synthetic
58
59
60

1
2
3 biodegradable polymers [22]. Natural polymers are known as the first clinically used
4 degradable biomaterial, and due to their bioactive properties, they interact better with cells [23].
5
6 Natural polymers can be classified as proteins, polysaccharides, and polynucleotides [24].
7
8 Proteins can be listed as myosin, gelatin, collagen, fibrinogen, elastin, keratin, actin, and silk.
9
10 Polysaccharides can be listed as cellulose, chitin, amylose, dextran, and glycosaminoglycans
11
12 and polynucleotides are DNA and RNA [24]. Synthetic polymers are advantageous in the
13
14 biomedical field because of their pore structures, tunable degradation properties, and
15
16 mechanical properties [25]. Polylactic acid (PLA), polyglycolic acid (PGA), and polylactic-co-
17
18 glycolic acid (PLGA) copolymers [26] and Polyhydroxyalkanoates (PHA) included in the
19
20 microbial polyester class are frequently used in tissue engineering [27].
21
22
23
24
25

26 It is essential to meet two requisites in the cellular approach of tissue engineering. The first is
27
28 that the cells integrate themselves into specific tissues, and the second is to secrete various
29
30 growth factors and cytokines that activate endogenous tissue regeneration. Therefore,
31
32 embryonic stem cells (ESC) and adult stem cells (ASC) are used as alternative cell sources in
33
34 tissue engineering [28]. ESCs are very limited in use due to their potential to produce teratomas
35
36 and are pluripotent cells that can be divided into many origins [29].
37
38
39

40 ASC and their derived tissues are less likely to be rejected after transplantation, and it has been
41
42 made possible to isolate these from different tissues such as bone, muscle and adipose tissue,
43
44 umbilical cord. Another cell type is pluripotent stem cells (iPSC), produced from mouse
45
46 fibroblasts and/or adult human cells. These cells have the advantage of autologous properties,
47
48 differentiation capacities and must understand the mechanisms underlying reprogramming
49
50 before implementation [30].
51
52

53 Hydrogels are the 3D network of cross-linked hydrophilic polymers that can hold large amounts
54
55 of water and exhibit an elastic behaviour due to their soft structure [31]. Pores allow diffusion
56
57 of biomolecules, nutrients, and oxygen and enable the release of cell metabolites and toxins
58
59
60

1
2
3 [32]. Hydrogels with a pore diameter of less than 10 μm have dense crosslinks and limit the
4
5 movement of the cell. The intense cross-links reduce the expansion of the gel and stabilize the
6
7 structure [33]. If the cross-links in the gel are chemical cross-links formed by the covalent bond,
8
9 it adds mechanical strength to the structure, and the gel exhibits elastic behaviour [34]. Physical
10
11 cross-linking is based on non-covalent interactions and allows stress release by demonstrating
12
13 viscoelastic gel behaviour [35].
14
15

16 17 **3. Properties and fabrication of hydrogels for corneal stroma applications**

18
19 A standard corneal scaffold should be designed to be transparent in the visible region,
20
21 mechanically strong, biocompatible, and allow cells to adhere, migrate and grow [35], which
22
23 are summarized in Figure 2. To date, synthetic and/or natural biomaterials in different forms
24
25 such as films [36], foams [37], 3D printed scaffolds [38] and decellularized tissues [39] have
26
27 been used to manufacture the cornea. Although some of the corneal structures are being
28
29 examined in Phase I clinical works [40], no corneal tissue-equivalent is available for standard
30
31 clinical use [41].
32
33

34
35 Advanced approaches have been developed to produce corneal equivalence based on natural
36
37 (collagen [42], gelatin [43], chitosan [44], silk [45] or synthetic materials (poly (ethylene
38
39 glycol) (PEG) [46], poly (ϵ -caprolactone) (PCL) [47], PLGA [41], poly-hydroxyethyl
40
41 methacrylate (PHEMA) [48]) or their combinations, using casting [49], hydrogel [50], 3D
42
43 printing [51], electrospinning processes [52], or their combinations [51]. Hydrogels from
44
45 natural materials [53] used in the production of corneal tissue have many advantages such as
46
47 biocompatibility, intrinsic cell-binding sites, 3D high pore structure, and a high degree of the
48
49 aqueous environment, as well as weak mechanical stability. Hydrogels from synthetic materials
50
51 have better mechanical stability while exhibiting worse biocompatibility [45]. Therefore,
52
53 chemically functionalized semi-synthetic hydrogels (gelatin methacrylate (GelMA)) have been
54
55
56
57
58
59
60

1
2
3 developed to obtain hydrogels that exhibit both mechanical stability and high biocompatibility
4
5 [54].
6

7 Fiber-reinforced hydrogels have been developed for application in soft tissue regeneration [55].
8
9

10 The fibers in the structure can increase the mechanical performance of the structure by sharing
11 the load on the hydrogels, and the mechanical stability can be easily compared to the mechanical
12 stability of the fibers obtained by the electrospinning method.
13
14
15

16 17 **4. Current 3D-printing techniques for bioinks design**

18
19 The 3D method allows building complex structures without using traditional molds [56]. In
20 recent years, 3D printing technologies have been widely used in various fields, including
21 aerospace, tissue engineering, architectures, etc. In particular, 3D bioprinting precisely controls
22 the accumulation of bioinks which consist of biomaterials and living cells [57]. The 3D printing
23 methods are fused deposition modelling (FDM), selective laser sintering (SLS), inkjet printing,
24 and stereolithography, etc [58].
25
26
27
28
29
30
31
32

33 **4.1. Fused deposition modelling(FDM)**

34
35 FDM technique consists of a filament made up of thermoplastic polymer. In this method, the
36 temperature was used for heating the filament to attain a semi-liquid state. Then, materials
37 extruded on the panel to build the layers. The thermoplastic property of the filament is an
38 excellent advantage for the FDM technique because filaments fuse during printing and easily
39 solidify at room temperature after printing. During printing, parameters such as layer thickness,
40 width, direction, air gaps between layers of the filaments affect the mechanical properties of
41 the product. The advantages of the FDM method include low cost, high speed and simplicity.
42 Its disadvantages are poor mechanical properties, low surface quality and the scarcity of
43 thermoplastic materials [58].
44
45
46
47
48
49
50
51
52
53
54

55 **4.2. Selective laser sintering(SLS)**

1
2
3 This technique uses a laser to bind powder particles together instead of using a sputtering
4 solution. A certain pattern is drawn on the surface of the powder bed with a laser. When the
5 first layer is formed, the roller distributes a new powder layer over the previous layer. Thus, the
6
7
8
9
10 object is produced layer by layer and then removed from under the powder bed. The materials
11
12 used for this technique are powdered plastic, ceramics, and metal alloys that require high
13
14 temperature and high energy laser [59]. While the SLS procedure is conceptually simple, the
15
16 underlying physics is complex and covers a wide variety of time and length scales [60].
17
18

19 **4.3. Inkjet printing**

20
21 The inkjet head prints a liquid binder onto fine powder layers based on object profiles created
22
23 by the software. The inkjet head prints a liquid binder onto fine powder layers based on object
24
25 profiles created by the software. Piezoelectric and thermal heads are used in inkjet systems.
26
27 Thermal heads have a heating element as a thin film resistor. When an electric shock is applied
28
29 to the thermal head, high current flows through this resistor, and the liquid on contact
30
31 evaporates, creating a vapor bubble on the resistor. This vapor bubble expands in the liquid
32
33 chamber, and the increased pressure causes the droplet to be ejected from the needle. In the
34
35 piezoelectric system, the volumetric change in the fluid reservoir is induced by applying a
36
37 voltage to the piezoelectric element directly or indirectly connected to the fluid. With the
38
39 volumetric change that occurs, it causes pressure in the fluid and the formation of drops from
40
41 the nozzle [61].
42
43
44
45
46

47 **4.4. Stereolithography(SLA)**

48
49 In SLA technique, the liquid resin is placed in a liquid reservoir and relies on photocuring, in
50
51 which a positionally programmed laser is scanned on the resin surface to initiate
52
53 photopolymerization. This hardens the resin and turns it from liquid to solid, usually through a
54
55 chemical crosslinking process. The layered nature prevents the SLA printed products from
56
57 reaching the mechanical properties of their monolithic counterparts. One of the advantages of
58
59
60

1
2
3 SLA printing is that active additives cannot be added to the resin as long as they are miscible.
4
5 By crosslinking the resin, the extra components are simply trapped in the polymeric matrix [62].
6

7 **5. Characterization of bioprinted hydrogels for stroma tissue**

8
9
10 Some assembled hydrogels as a potential material for the cornea stroma layer was given in
11
12 Figure 3 and Table 2.
13

14 **5.1. Physical characterizations**

15
16 Understanding the physical possessions of gelled systems comprising emulsifying or stabilizing
17 factors becomes essential for developing the systems' properties [63]. Campos et al. [64]
18 created 3D corneal stromal models with drop-on-demand bioprinting. Bioink was formed with
19 a combination of corneal stromal keratocytes and collagen-based composite. In this study,
20 rotational rheometer was used to measure the rheological properties of non-printable 0.3% Type
21 I collagen and 3D-bioprintable 0.5% agarose with 0.2% collagen gel mixtures at 37 °C.
22 According to the results, they found that blended bioink had higher viscosity compared to the
23 pure collagen bioinks, and it had faster gelation time.
24
25

26
27 In the Kim et al. study [65], they built a biomimetic corneal stroma tissue containing corneal
28 decellularized extracellular matrix (Co-dECM) and cells by 3D bioprinting. Rheometric
29 Expansion System was used to analyse the rheological properties of 0.5%, 1.0%, 1.5%, and 2%
30 of Co-dECM gels. According to this study, Co-dECM gel with various concentrations showed
31 shear-thinning behaviours in 1-1000 s⁻¹ shear stress range, and larger viscosity values at 1 s⁻¹
32 shear rate were observed for Co-dECM gel which has a higher concentration. The viscosity
33 values were found as 2.35, 3.83, 22.51, and 64.99 Pa.s for 0.5, 1, 1.5, and 2.0 %Co-dECM,
34 respectively.
35

36
37 Kutlehria et al. [66] fabricated cornea stroma using 3D bioprinting. In this study, sodium
38 alginate, gelatin type B, and type I collagen solution were combined to fabricate the cornea
39 stroma. The rheometer was used to investigate the rheological behaviours of the gels. According
40
41
42
43
44
45
46
47
48
49
50
51
52
53
54
55
56
57
58
59
60

1
2
3 to their results, gelatin melted at the printing temperature higher than 37° C and storage modulus
4 of the bio-ink decreased above this temperature value. Printing temperature lower than 20° C
5
6 caused the high-pressure requirement to extrude the filament.
7
8

9 **5.2. Swelling/degradation behaviours**

10
11
12 Corneal swelling is related to the electrostatic repulsion between matrix charges connected to
13 other collagen fibrils [67].
14

15
16 In Bektas et al. study, transparent Gelatin Methacryloyl (GELMA) hydrogel was fabricated.
17
18 Corneal stromal keratocytes were loaded into hydrogels and printed using extrusion-based
19 bioprinter. In this study, the water intake capacity of the produced hydrogel was measured at
20 certain intervals by keeping the hydrogel in body fluid with 0.5 mg/mL sodium azide at 37 °C.
21
22 They found that hydrogels absorbed a notable amount of water (90%) into their structures [68].
23
24
25

26
27 In Ulag et al. work, cornea stroma tissue was fabricated with a combination of Polyvinyl alcohol
28 (PVA) and Chitosan (CS) using 3D printing. According to this procedure, PBS (pH=7) was
29 used to incubate the printed constructs using a thermoshaker at 37 °C in thermal shaker during
30 a week. The results indicated that constructs immersed PBS rapidly, and this continued up to a
31 constant swelling rate. The swelling ratio of CS added composites was higher than
32 13%(wt)PVA matrix [69].
33
34
35

36
37 Bektas et al. observed the degradation properties of GELMA hydrogels, with and without
38 enzymatic degradation. According to their methods, hydrogels were frozen dried to report their
39 initial weights, and they were incubated in 10 mM PBS (pH 7.4) for 3 weeks, shaking at 37 °C.
40
41 The samples were then rinsed with distilled water, lyophilized and weighted for 1, 7, 14, and
42 21 days. They performed the degradation test with collagenase type II. Prewighted samples
43 were incubated in solutions which contained 1, 2.5, 5, and 10 U collagenase Type II/ml in PBS
44 (7.4) for 4 hours. According to their results, 3D printed hydrogels lost their weights within the
45 21 days [68].
46
47
48
49
50
51
52
53
54
55
56
57
58
59
60

1
2
3 In Ulag et al. study, degradation behaviours of the 13%wtPVA/(1, 3, 5)wt.%CS cornea stroma
4 constructs were observed in PBS for a month. During the test, fresh PBS was used. All
5 constructs absorbed the PBS until 3 days, and after this time they started to lose their weights.
6
7
8
9
10 With CS addition, the degradation rate increased, and 13%PVA/5%CS had higher degradation
11 value [69].
12
13

14 **5.3. Porosity analyses**

15
16
17 Mahdavi et al. study, GELMA hydrogels were produced with 7.5 and 12.5 % concentrations
18 and mixed with corneal stromal cells using stereolithography bioprinting. SEM was used to
19 examine the microstructure of GELMA hydrogels. ImageJ software using a built-in threshold
20 and particle functions analysis was used to measure the porosity. According to their results,
21
22
23
24
25
26
27
28
29
30
31
32
33
34
35
36
37
38
39
40
41
42
43
44
45
46
47
48
49
50
51
52
53
54
55
56
57
58
59
60

31 **5.4. Permeability Analyses**

32
33
34
35
36
37
38
39
40
41
42
43
44
45
46
47
48
49
50
51
52
53
54
55
56
57
58
59
60

47 **5.5. Morphological analyses**

48
49
50
51
52
53
54
55
56
57
58
59
60

1
2
3 In Kutlehria et al. [66], before the SEM imaging, polydimethylsiloxane (PDMS) corneal
4 substitutes were got ready with silicone elastomer base and silicone elastomer curing agent in
5 a 10: 1 ratio, respectively. They were centrifugated to remove bubbles. After that, the samples
6 were put in an oven for 12 hr, 9° C. The PDMS corneas were then discarded from the wells.
7
8
9
10
11
12 PDMS sample was mounted, and SEM images were captured by Helios G4 UC at 2 kV.

13 14 15 **5.6. Transparency properties**

16
17 The optical property is an essential parameter for corneal transplantation [68]. In Bektas et al.
18 study [68], cell-loaded (1×10^6 cells) and cell-free GELMA hydrogels were analyzed in the
19 range of 250-700 nm wavelength with a UV spectrophotometer on days 1, 7, 14, and 21. They
20 observed nearly 75% transmittance value for cell loaded hydrogels on day 1 at 700 nm. With
21 the increase of culture time, the transmittance of the hydrogels increased to around 83%. During
22 three weeks in culture, the transparency of cell-free and cell-loaded hydrogels exhibited 80%
23 value, which is closed to the transparency value of the innate cornea (85%). In Ulag et al., light
24 transmittance percentage of the 3D-printed stroma constructs was determined using UV/VIS
25 Spectrophotometer in the visible region, and with Chitosan addition, transmittance values
26 decreased a bit [69].

27
28
29
30
31
32
33
34
35
36
37
38
39
40 Kim et al. produced bioinks which have decellularized corneal extracellular matrix (Co-dECM)
41 hydrogel and differentiated keratocytes [65]. The light transmittance measurement was tested
42 using a microplate reader. The native human cornea was determined as a control group, and
43 they were dehydrated in glycerol. 200- μm thickness value was determined for all samples, and
44 the test was performed in the range of 300-700 nm wavelength.

45
46
47
48
49
50
51 In Mahdavi et al. study, Gelatin Methacrylate (GELMA) was combined with corneal stromal
52 cells to fabricate bioink for stroma equivalent. The transparency properties were tested after
53 cell encapsulation into the bioprinted three-dimensional scaffolds for 1, 3, and 7 days. ELISA
54
55
56
57
58
59
60

1
2
3 microplate reader was utilized to determine the absorbance of the samples at 450, 490, 570 and
4
5 630 nm.

6
7 Transmission spectrum was recorded for both the edge and center of the bioprinted samples.

8
9 Results showed that native cornea tissue had different transmittance values ranging from 80 to
10
11 94% in the 450 to 600 nm wavelength and 95 to 98% in the 600-1000 nm. The produced 12.5%
12
13 GELMA had optical transmittance values of 80-95% at the edge and 78-90% at the centre. 7.5%
14
15 GELMA showed lower transmittance value compared to the native corneal tissue [70].

16
17 Kim et al. fabricated stroma containing corneal decellularized extracellular matrix (Co-dECM)
18
19 gel encapsulated with cells. The transparency of the samples was examined using a microplate
20
21 reader at 300-700 nm range. Samples were produced with 25GN (25 Gauge Nozzle), and PG
22
23 (non-printed group) were put into the 48-well plate to provide the same height of native cornea,
24
25 which is about 500 μm . After that, samples were cultured for 28 days in white media. According
26
27 to the results, 25GN showed more transparency than PG, which value is similar to the native
28
29 cornea (over than 75%). The aligned cells in 25GN increase the light to transmit the human
30
31 cornea [65].

32
33 In the study of Kutlehria et al. [66], light transmittance values were determined from the
34
35 microplate reader at 300-700 nm range. Before the measurement, bioink was solved at 37 °C
36
37 and poured into a 48-well plate to match the thickness and height values of the human cornea.
38
39 Results showed that the transmittance of inks was a range from 75% to 90%.

40 41 42 **5.7. Mechanical characterizations**

43
44 Compression test was performed using 5 N load and displacement rate of 1 mm/min, in Bektas
45
46 et al. study. According to the results, modulus of compression of the GelMA hydrogels was
47
48 lower than the mechanical strength of the native corneas (403 to 624 kPa) but still had the
49
50 potential [68].
51
52
53
54
55
56
57
58
59
60

1
2
3 In Ulag et al. study, the mechanical properties of the dry 3D-bioprinted constructs were
4 determined by the tensile testing device. Degrade samples were also included in tensile testing
5 to analyze the mass loss effect on mechanical possessions. In this study, samples had sufficient
6 mechanical strength even if they lose their masses [69].
7
8
9

10
11
12 Unconfined compression testing was used in Campos et al. study [65] to determine the stiffness
13 of Collagen tip I and agarose bioinks. Samples were pressed at a cross-speed of 4 mm/min onto
14 the testing platform until rupture. It was reported that compressive modulus of the mixture
15 bioink was 18.1 ± 3.5 kPa. The compressive modulus for the human cornea is ~ 300 kPa [69].
16
17
18

19 **5.8. *In vitro* cell viability**

20
21
22 In Sorkio et al. study [37], the authors fabricated three types of corneal layers, stratified corneal
23 epithelium using human embryonic stem cell-limbal epithelial stem cells (hESC-LESCs),
24 lamellar corneal stroma using acellular layers of bioink and hASCs, and constructs with both a
25 stromal and epithelial part. The hESC-LESC viability was performed after 3 and 7 days of
26 printing, next day cell viability of hASCs was examined. The PrestoBlue™ viability assay
27 was carried out on 1 and 7 days for hESC-LESCs, 1 and 4 days for hASCs printed in 2D models.
28 For 3D stromal mimicking structures, they cultured at 1, 4, and 7 days.
29
30
31
32

33
34
35 According to the protocol of the Ulag et al. study, MTT procedure was carried out for 1, 3, and
36 7 days for corneal structures. Printed cornea constructs with 4×10^4 hASCs and DMEM were
37 incubated together for 30 min, at 37 °C, 5%CO₂.
38
39

40
41
42 To observe the cytotoxic properties of the cornea constructs, cytotoxicity detection kit was used.
43 ELISA reader was used for measuring the absorbance values at 560 nm wavelength. MSCs
44 morphologies on the 3D-printed constructs were observed under a fluorescence microscope and
45 SEM [69].
46
47
48

49
50
51 In Campos et al. study [65], CSKs was used to examine the live/dead cells on the 3D-bioprinted
52 Collagen tip I and agarose bioinks. First, cells (10^6 cells) were trypsinized and embedded in
53
54
55
56
57
58
59
60

1
2
3 bioinks supplemented with 0.5% agarose with 0.2% Collagen type I. After one and seven days
4
5 of the bioprinting, live/dead marking was visualized with a laser scanning microscope. To see
6
7 the CSK survival after the bioprinting process, the constructs were incubated at 37 °C for 1 and
8
9 7 days. After incubation, it was observed that most cells were live. Immunocytochemical
10
11 stainings were carried out with antibodies identifying human keratocan, lumican, and smooth
12
13 muscle actin to sustain the phenotype of CSK in 3D-bioprinted inks. They observed that CSK
14
15 in bioinks elongated parallel to each other to resemble the innate cornea.
16
17

18
19 In Bektas et al. study [68], live-dead human corneal keratocytes (HCKs) viability assay was
20
21 performed on the GELMA discs for 1, 2, 7, and 21 days. ImageJ program was utilized to
22
23 calculate the live/dead keratocytes in the hydrogels. In the immunofluorescence staining,
24
25 Collagen Types I/V, decorin, and biglycan antibodies were used. The samples were incubated
26
27 at 4 °C with these antibodies during the night. Samples were rinsed and incubated with either
28
29 anti-rabbit or anti-mouse Alexa fluor 488 secondary antibodies. Then, nuclei of the cells were
30
31 marked with DRAQ5 at RT and incubated for 1 hr. Samples were stored in PBS for CLSM
32
33 examination.
34
35

36
37 Kutlehria et al. [66] performed human corneal keratocytes (HCKs) viability for sodium
38
39 alginate/gelatin/collagen bioinks for days 1, 7, and 14 live/dead assay. Live/dead assay
40
41 contained the calcein and ethidium bromide II with a ratio of 1:4. After that, live/dead solution
42
43 was added to printed corneas, and the plate was incubated at 37° C for half an hour. Image J1
44
45 program was used to calculate the cell viability.
46
47

48
49 To observe the cell number/growth, Alamar blue assay was carried out in Kutlehria et al. study.
50
51 First of all, HBSS was used to wash the corneas, then 10% Alamar blue was added into the
52
53 wells. After that, the plates were placed inside the incubator for 4 hr at 37° C and 5%CO₂. The
54
55 concentration was analyzed at 560 nm, 590 nm, and 570 nm using a plate reader. The same
56
57
58
59
60

1
2
3 protocol was used for 1, 10, and 14 days. They reported that high cell viability observed for the
4
5 optimal combination of collagen, gelatin [66].
6

7 **6. *In vivo* evaluations**

8
9
10 Sorkio et al. [38] tested the corneal structures *in vivo* into organ cultured porcine model. To
11
12 prepare the porcine corneas for the experiment, the corneas were removed from the eyes in
13
14 aseptic disciplines. CnT-Prime-CC medium supplemented with 1%Penicillin-Streptomycin
15
16 amphotericin B and Plasmocin was used to culture the corneas at 37 °C, 5%CO₂ for two weeks
17
18 before the transplantation. Two-day-old 3D printed stromal structures were implanted into the
19
20 corneal organ cultures 4 days after printing. After implantation, the corneas were moved back
21
22 to the culture plates, covered with soft contact lenses, and partially immersed in EBM-2 medium
23
24 with 2% HS for 7 days at +37 ° C in 5% CO₂. One week after implantation, corneal organ
25
26 cultures were fixed in 4% PFA for 4 hours at room temperature, dehydrated in the Tissue-Tek
27
28 VIP 5 automated tissue processor and embedded in paraffin. Paraffin blocks were cut into 6
29
30 mm thick slices and the sections were viewed with a microscope. According to the results, 3D-
31
32 bioprinted stromal constructs demonstrated interaction to the host tissue and 3D bioprinted
33
34 structures showed good mechanical robustness after implantation to the corneal culture model
35
36 after 7 days of implantation.
37
38
39

40
41
42 In Kim et al. research [65], they performed the animal experiment to observe the transparency
43
44 *in vivo* with Ten healthy New Zealand white rabbits. Anesthesia was performed using ketamine
45
46 (15 mg/mL) and rompun (5 mg/mL). Three-quarter circular sections of 6 mm in diameter were
47
48 taken with a crescent-shaped blade. Five printed and five NP samples were transplanted into
49
50 the corneal stroma of each animal. The incision areas were sutured with ethylon nylon and the
51
52 operated eyes were treated with eye drops containing polymyxin B, neomycin and
53
54 dexamethasone twice a day for 2 weeks. Then they were intramuscularly injected with ketamine
55
56 and rompun; gently placed on the sample stage of a medical kit, and kept there for 10 min prior
57
58
59
60

1
2
3 to the experiment. To obtain micro-dust-particles-free OCT image, we washed the eyes with
4
5 physiological saline to remove foreign substances, dust particles, and eyebrows. The
6
7 experiments were carried out for 2 weeks. According to their results, the 25G implanted
8
9 cornea had more transparency compared to the NP implanted cornea. Furthermore, it was
10
11 reported that all transplanted constructs were incorporated with the surrounding corneal tissue
12
13 for 28 days and after *in vivo* transplantation, no enzymatic degradation of the collagen was
14
15 found.
16
17

18 19 **7. Conclusion and future outlook**

20
21 The stroma is the key and thickest layer in the cornea. There have been valuable efforts on the
22
23 direction of useful and biocompatible stromal transplantation. Each study has its advantages
24
25 and disadvantages, and as with all areas of tissue engineering, *in vitro*, results do not often
26
27 indicate good *in vivo* behaviour. The aforementioned characterization techniques have been
28
29 valuable supports to the application of corneal stroma engineering. Future research should focus
30
31 on combining various techniques to succeed adequate stromal replacements and regenerate the
32
33 functionality of the stroma.
34
35

36 37 **Acknowledgements**

38
39 The authors, thanks to Marmara University Scientific Research Committee (FDK-2020-10117)
40
41 for their support. DMK would like to thank bioprinting platform grant by UKIERI
42
43 (IND/CONT/G/17-18/46) for international collaboration.
44
45

46 47 **References**

- 48
49 [1] Ludwig PE, Lopez MJ. Anatomy, Head and Neck, Eye Cornea. StatPearls, 2020.
50
51 [2] Chen Z, You J, Liu X, Cooper S, Hodge C. Biomaterials for corneal bioengineering.
52
53 Biomedical Materials. 2018, 13 (3): 032002.
54
55 [3] Sridhar MS. Anatomy of cornea and ocular surface. Indian J. Ophthalmol. 2018, 66: 190–
56
57 194.
58
59
60

- 1
2
3 [4] DelMonte DW, Kim T. J. Anatomy and physiology of the cornea. *Cataract Refract. Surg.*
4 2011, 37 (3): 588–598.
5
6
7 [5] Islam MM, Sharifi R, Gonzalez-Andrades M. *Corneal Tissue Engineering*. Springer Cham,
8 2019.
9
10
11 [6] Ghezzi CE, Rnjak-Kovacina J, Kaplan DL. Corneal tissue engineering: recent advances and
12 future perspectives. *Tissue Eng. Part B Rev.* 2015, 21 (3): 278–287.
13
14
15 [7] Yousaf S, Keshel SH, Farzi GA, Momeni-Moghadam M, Ahmadi ED, Asencio IO,
16 Mozafari M, Sefat F. *Scaffolds for corneal tissue engineering*. Woodhead Publishing Series in
17 Biomaterials, 2019, 649-672.
18
19
20 [8] Matthyssen S, Van den Bogerd B, Dhubhghaill SN, Koppen C, Zakaria N. Corneal
21 regeneration: A review of stromal replacements. *Acta Biomater.* 2018, 69: 31–41.
22
23
24 [9] Marshall GE, Konstas AG, Lee WR. Graefe's Arch. Immunogold fine structural localization
25 of extracellular matrix components in aged human cornea. *Clin. Exp. Ophthalmol.* 1991, 229
26 (2): 157–163.
27
28
29 [10] Maurice DM. The transparency of the corneal stroma. *Vision Res.* 1970, 10 (1): 107–108.
30
31
32 [11] Farrell R, McCally R. Corneal transparency, in *Principles and Practice of Ophthalmology*.
33 Philadelphia: WB Saunders, 2000, 629–643.
34
35
36 [12] Chaurasia SS, Lim RR, Lakshminarayanan R, Mohan RR. Nanomedicine approaches for
37 corneal diseases. *J. Funct. Biomater.* 2015, 6 (2): 277-98.
38
39
40 [13] Whitcher JP, Srinivasan M, Upadhyay MP. Bull. Corneal blindness: a global perspective.
41 World Health Organ. 2001, 79 (3): 214–221.
42
43
44 [14] Williams KA, Lowe M, Bartlett C, Kelly TL, Coster DJ. Risk factors for human corneal
45 graft failure within the Australian corneal graft registry. *Transplantation* 2008, 86 (12): 1720–
46 1724.
47
48
49
50
51
52
53
54
55
56
57
58
59
60

- 1
2
3 [15] Tan DTH, Dart JKG, Holland EJ, Kinoshita S. Corneal transplantation. *Lancet*, 2012, 379:
4 1749–1761.
5
6
7 [16] Eye Banking Statistical Report, EBAA, no. 202. 2016.
8
9
10 [17] Palchesko RN, Carrasquilla SD, Feinberg AW. Palchesko RN, et al. In vitro expansion of
11 corneal endothelial cells on biomimetic substrates. *Sci Rep*. 2015;5:7955. *Adv. Healthc. Mater.*
12 2018, 7 (16): 1–18.
13
14
15 [18] Akpek EK, Alkharashi M, Hwang FS, Ng SM, Lindsley K. Artificial corneas versus donor
16 corneas for repeat corneal transplants. *Cochrane Database Syst. Rev*. 2014, 11 (11): 1–31.
17
18
19 [19] Fagerholm P, Lagali NS, Merrett K, Jackson WB, Munger R, Liu Y, Polarek JW,
20 Söderqvist M, Griffith M. A Biosynthetic Alternative to Human Donor Tissue for Inducing
21 Corneal Regeneration: 24-Month Follow-Up of a Phase 1 Clinical Study. *Sci. Transl. Med.*
22 2010, 2 (46): 46-61.
23
24
25 [20] Shah A, Brugnano J, Sun S, Vase A, Orwin E. The Development of a Tissue-Engineered
26 Cornea: Biomaterials and Culture Methods. *Pediatr. Res*. 2008, 63 (5): 535–544.
27
28
29 [21] E. Piskin. Biodegradable polymers as biomaterials. *Journal of Biomaterials Science*
30 *Polymer Edition*, 1994, 6, 775–795.
31
32
33 [22] Ramakrishna S, Mayer J, Wintermantel E, Leong KW. Biomedical applications of
34 polymer-composite materials: A review. *Composites science and technology*, 2001, 61(9):
35 1189-1224.
36
37
38 [23] Nair LS, Laurencin CT. Biodegradable polymers as biomaterials. *Progress in Polymer*
39 *Science*, 2007, 32 (8-9): 762-798.
40
41
42 [24] Ratner BD, Hoffman AS, Schoen FJ, Lemons JE. *Biomaterials Science An Introduction to*
43 *Materials in Medicine* 2nd Edition. Eds. 2004, 127–136.
44
45
46 [25] Gunatillake P, Mayadunne R, Adhikari R. Recent developments in biodegradable synthetic
47 polymers. *Biotechnology Annual Review*, 2006, 12: 301.
48
49
50
51
52
53
54
55
56
57
58
59
60

- 1
2
3 [26] Ma PX. Scaffolds for tissue fabrication. *Materials Today*, 2004, 7 (5): 30-40.
4
5 [27] Chen LJ, Wang M. Production and evaluation of biodegradable composites based on PHB-
6
7 PHV copolymer. *Biomaterials*, 2002, 23 (13): 2631-2639.
8
9 [28] Bernstein HS, Srivastava D. Stem cell therapy for cardiac disease. *Pediatric research*, 2012,
10
11 71: 491–499.
12
13 [29] Naderi H, Matin MM, Bahrami AR. Review paper: critical issues in tissue engineering:
14
15 biomaterials, cell sources, angiogenesis, and drug delivery systems. *Journal of biomaterials*
16
17 applications, 2011, 26: 383-417.
18
19 [30] Zhu Z, Huangfu D. Human pluripotent stem cells: an emerging model in developmental
20
21 biology. *Development*, 2013, 140 (4): 705-717.
22
23 [31] El-Sherbiny IM, Yacoub MH. Hydrogel scaffolds for tissue engineering: Progress and
24
25 challenges. *Glob. Cardiol. Sci. Pract*, 2013, 3: 316-342.
26
27 [32] Khan F, Tanaka M, Ahmad SR. Fabrication of polymeric biomaterials: a strategy for tissue
28
29 engineering and medical devices. *J. Mater. Chem. B*, 2015, 3(42): 8224 8249.
30
31 [33] Slaughter BV, Khurshid SS, Fisher OZ, Khademhosseini A, Peppas NA. Hydrogels in
32
33 regenerative medicine. *Adv. Mater.* 2009, 21: 3307-29.
34
35 [34] Huang Q, Zou Y, Arno MC, Chen S, Wang T, Gao J, Dove AP, Du J. Hydrogel scaffolds
36
37 for differentiation of adipose-derived stem cells. *Chem. Soc. Rev.* 2017, 46 (20): 6255–6275.
38
39 [35] Lin L, Jin X. The development of tissue engineering corneal scaffold: which one the history
40
41 will choose? *Ann Eye Sci.* 2018, 3:1.
42
43 [36] Kilic C, Girotti A, Rodriguez-Cabello JC, Hasirci V. A collagen-based corneal stroma
44
45 substitute with micro-designed architecture. *Biomater Sci.* 2014, 2: 318-329.
46
47 [37] Vrana NE, Builles N, Justin V, Bednarz J, Pellegrini G, Ferrari B, Damour O, Hulmes DJS,
48
49 Hasirci V. Development of a Reconstructed Cornea from Collagen–Chondroitin Sulfate Foams
50
51 and Human Cell Cultures. *Invest Ophthalmol Vis Sci.* 2008, 49: 5325-5331.
52
53
54
55
56
57
58
59
60

- 1
2
3 [38] Sorkio A, Koch L, Koivusalo L, Deiwick A, Miettinen S, Chichkov B, Skottman H. Human
4 stem cell based corneal tissue mimicking structures using laser-assisted 3D bioprinting and
5 functional bioinks. *Biomaterials*, 2018, 171: 57-71.
6
7
8
9
10 [39] Márquez SP, Martínez VS, Ambrose WM, Wang J, Gantxegui NG, Schein O, Elisseff J.
11 Decellularization of bovine corneas for tissue engineering applications. *Acta Biomater*. 2009,
12 5 (6): 1839-47.
13
14
15
16 [40] Fagerholm P, Lagali NS, Merrett K, Jackson WB, Munger R, Liu Y, Polarek JW,
17 Söderqvist M, Griffith M. A Biosynthetic Alternative to Human Donor Tissue for Inducing
18 Corneal Regeneration: 24-Month Follow-Up of a Phase 1 Clinical Study. *Sci Transl Med*. 2010,
19 2 (46): 46-61.
20
21
22
23
24
25 [41] Bektas CK, Hasirci V. Cell Loaded GelMA: HEMA IPN hydrogels for corneal stroma
26 engineering. *Journal of Materials Science: Materials in Medicine*, 2020, 31(2): 6345-4.
27
28
29 [42] Kong B, Sun W, Chen G, Tang S, Li M, Shao Z, Mi S. Tissue-engineered cornea
30 constructed with compressed collagen and laser-perforated electrospun mat. *Sci. Rep*. 2017, 7
31 (1): 970–983.
32
33
34
35
36 [43] Luo LJ, Lai JY, Chou SF, Hsueh YJ, Ma DH. Development of gelatin/ascorbic acid
37 cryogels for potential use in corneal stromal tissue engineering. *Acta Biomater*. 2017, 65: 123-
38 136.
39
40
41
42
43
44 [44] Ozcelik B, Brown KD, Blendcowe A, Daniell M, Stevens GW, Qiao GG. Ultrathin
45 chitosan-poly(ethylene glycol) hydrogel films for corneal tissue engineering. *Acta Biomater*.
46 2013, 9: 6594-605.
47
48
49
50 [45] Lawrence BD, Marchant JK, Pindrus MA, Omenetto FG, Kaplan DL. Silk film
51 biomaterials for cornea tissue engineering. *Biomaterials*, 2009, 30 (7): 1299-308.
52
53
54
55
56
57
58
59
60

- 1
2
3 [46] Garagorri N, Fermanian S, Thibault R, Ambrose WM, Schein OD, Chakravarti S, Elisseeff
4 J. Keratocyte behavior in three-dimensional photopolymerizable poly(ethylene glycol)
5 hydrogels. *Acta Biomater.* 2008, 4 (5): 1139-1147.
6
7
8
9
10 [47] Then KY, Yang Y, Ahearne M, El Haj AJ. Effect of microtopographical cues on human
11 keratocyte orientation and gene expression. *Curr. Eye Res.* 2011, 36 (2): 88–93.
12
13 [48] Wang L, Lu C, Liu H, Lin S, Nan K, Chen H, Li L. A double network strategy to improve
14 epithelization of a poly(2-hydroxyethyl methacrylate) hydrogel for corneal repair application.
15 RSC Adv. 2016, 6: 1194-1202.
16
17
18
19 [49] Wang SR, Ghezzi CE, Gomes R, Pollard RE, Funderburgh JL, Kaplan DL. In vitro 3D
20 corneal tissue model with epithelium, stroma, and innervation. *Biomaterials* 112, 1–9.
21 *Biomaterials*, 2017, 112.
22
23
24 [50] Rizwan M, Peh GS, Ang HP, Lwin NC, Adnan K, Mehta JS, Yim EK. Sequentially-
25 crosslinked bioactive hydrogels as nano-patterned substrates with customizable stiffness and
26 degradation for corneal tissue engineering applications. *Biomaterials*, 2016, 120: 139-154.
27
28
29 [51] Wu Z, Su X, Xu Y, Kong B, Sun W, Mi S. Bioprinting three-dimensional cell-laden tissue
30 constructs with controllable degradation. *Sci. Rep.* 2016, 6: 24474.
31
32
33 [52] Wilson SL, Wimpenny I, Ahearne M, Rauz S, El Haj AJ, Yang Y. Chemical and
34 Topographical Effects on Cell Differentiation and Matrix Elasticity in a Corneal Stromal Layer
35 Model. *Adv. Funct. Mater.*, 2012, 22 (17): 3641-3649.
36
37
38 [53] Rafat M, Xeroudaki M, Koulikovska M, Sherrell P, Groth F, Fagerholm P, Lagali N.
39 Composite core-and-skirt collagen hydrogels with differential degradation for corneal
40 therapeutic applications. *Biomaterials*, 2016, 83: 142-55.
41
42
43 [54] Chen YC, Lin RZ, Qi H, Yang Y, Bae H, Melero-Martin JM, Khademhosseini A.
44 Functional Human Vascular Network Generated in Photocrosslinkable Gelatin Methacrylate
45 Hydrogels. *Adv. Funct. Mater.* 2012, 22 (10): 2027-2039.
46
47
48
49
50
51
52
53
54
55
56
57
58
59
60

- 1
2
3 [55] O. Bas, Catelas I, De-Juan-Pardo EM, Hutmacher DW. The quest for mechanically and
4 biologically functional soft biomaterials via soft network composites. *Adv. Drug Delivery Rev.*
5 2018, 132: 214-234.
6
7
8
9
10 [56] Li H, Tan C, Li L. Review of 3D printable hydrogels and constructs. *Materials & Design*,
11 2018, 159 (5): 20-38.
12
13
14 [57] Tan JY, Tan X, Yeong WY, Tor SB. Hybrid micro scaffold-based 3D bioprinting of multi-
15 cellular constructs with high compressive strength: a new biofabrication strategy. *Sci. Rep.*,
16 2016, 6.
17
18
19
20
21 [58] D.Ngoa T, Kashania A, Imbalzano G, Nguyen KTQ, Hui D. Additive manufacturing (3D
22 printing): A review of materials, methods, applications and challenges. *Composites Part B:*
23 *Engineering*, 2018, 143: 172-196.
24
25
26
27
28 [59] Fina F, Goyanes A, Gaisford S, Basit AW. Selective laser sintering (SLS) 3D printing of
29 medicines. *International Journal of Pharmaceutics*, 2017, 529 (1–2): 285-293.
30
31
32
33 [60] Yang Y, Ragnvaldsen O, Bai Y, Yi M, Xu BX. 3D non-isothermal phase-field simulation
34 of microstructure evolution during selective laser sintering. *Comput Mater* 5, 2019, 81.
35
36
37 [61] Shirazi SFS, Gharekhani S, Mehrali M, Yarmand H, Metselaar HSC, Kadri NA, Osman
38 NAA. A review on powder-based additive manufacturing for tissue engineering: selective laser
39 sintering and inkjet 3D printing. *Sci. Technol. Adv. Mater*, 2015, 16: 033502.
40
41
42
43
44 [62] Manapat JZ, Chen Q, Ye P, Advincula, RC. 3D Printing of Polymer Nanocomposites via
45 Stereolithography. *Macromol. Mater. Eng.* 2017, 302 (9): 1600553.
46
47
48
49 [63] Cuomo F, Cofelica M, Lopez F. Rheological Characterization of Hydrogels from Alginate-
50 Based Nanodispersion. *Polymers*, 2019, 11(2): 259.
51
52
53
54 [64] Campos DFD, Rohde M, Ross M, Anvari P, Blaeser A, Vogt M, Panfil C, Yam GHF,
55 Mehta JS, Fischer H, Walter P, Fuest M. Corneal bioprinting utilizing collagen-based bioinks
56 and primary human keratocytes. *J Biomed Mater Res*, 2019, 107A:1945–1953.
57
58
59
60

- 1
2
3 [65] Kim H, Jang J, Park J, Lee KP, Lee S, Lee DM, Kim KH, Kim HK, Cho DW. Shear-
4 induced alignment of collagen fibrils using 3D cell printing for corneal stroma tissue
5 engineering. *Biofabrication*, 2019, 1-23.
6
7
8
9
10 [66] Kutlehria S, Dinh TC, Bagde A, Patel N, Gebeyehu A, Singh M. High-throughput 3D
11 bioprinting of corneal stromal equivalents. *J Biomed Mater Res*, 2020, 108B:2981–2994.
12
13 [67] Hodson S, Earlam R. High-throughput 3D bioprinting of corneal stromal equivalents.
14 *Journal of Theoretical Biology*, 1993, 163 (2): 173-180.
15
16 [68] Bektas CK, Hasirci V. Cell loaded 3D bioprinted GelMA hydrogels for corneal stroma
17 engineering. *Biomater. Sci*, 2020, 8, 438–449.
18
19 [69] Ulag S, Ilhan E, Sahin A, Yilmaz BK, Ekren N, Kilic O, Oktar FN. 3D printed artificial
20 cornea for corneal stromal transplantation. *European Polymer Journal*, 2020, 133: 109744.
21
22 [70] Mahdavi SS, Abdekhodaie MJ. Stereolithography 3D Bioprinting Method for Fabrication
23 of Human Corneal Stroma Equivalent. *Annals of Biomedical Engineering*, 2020, 48 (7): 1955–
24 1970.
25
26
27
28
29
30
31
32
33
34
35
36
37
38
39
40
41
42
43
44
45
46
47
48
49
50
51
52
53
54
55
56
57
58
59
60

FIGURES/TABLE LEGEND

Figure 1. Schematic view of the cornea and its fundamental layers with details

Figure 2. The schematic view of the required properties of hydrogels.

Figure 3. The eye (a), gel (b), cell (c), bioprinting device (d), images of fabricated 3D-bioprinted corneas (e-j): gelatin type B/sodium alginate/type I collagen (e), 3D bioprinted GELMA hydrogel (f), 3D bioprinted collagen based bioink (g), PVA/CS cornea stroma construct (h), 3D printed GELMA hydrogel (i), CSK loaded bioprinted stroma (j).

Table 1. The suitable biomaterials for cornea tissue replacement.

Table 2. Summary of recent developments of 3D-bioprinted corneal stroma structures, properties, and characterization techniques in the literature.